Dissipative dynamics of a charged particle in the field of three plane waves: chaos and control

Ricardo Chacón
Departamento de Electrónica e Ingeniería Electromecánica, Escuela de Ingenierías Industriales, Universidad de Extremadura, Apartado Postal 382, E-06071 Badajoz, Spain

(Dated: February 8, 2008)

The chaotic dissipative dynamics of a charged particle in the field of three plane waves is theoretically (Melnikov's method) and numerically (Lyapunov exponents) investigated. In particular, the effectiveness of one of such waves in controlling the chaotic dynamics induced by the remaining two waves is theoretically predicted and numerically confirmed. Two mechanisms underlying the chaos-suppression scenario are identified. One mechanism requires chaos-inducing and chaos-suppressing waves to have both commensurate wavelengths and commensurate relative (with respect to the remaining third wave) phase velocities, while the other mechanism allows the chaotic dynamics to be tamed when such quantitites are incommensurate. The present findings may be directly applied to several important problems in plasma physics, including that of the chaos-induced destruction of magnetic surfaces in tokamaks.

PACS numbers: 52.40.Db, 05.45.Gg

The interaction of charged particles with a wave packet is a basic and challenging problem appearing in many fundamental fields such as astrophysics, plasma physics, and condensed matter physics [1,2], to name just a few. As is well known, the structure of the wave packet reflects the particular physical situation that is being considered in each case. In this regard, a classical, widely studied particular case is that of an infinite set of electrostatic waves having the same amplitudes and wave numbers, zero initial phases, and integer frequencies [3]. While the Hamiltonian approach to the general problem is suitable in many physical contexts [4], the consideration of dissipative forces seems appropriate so as to take into account such diverse phenomena as electron-ion collisions, energy losses through synchrotron radiation, and stochastic heating of particles in plasma physics. In any case, stochastic (chaotic) dynamics already appears (can appear) when the wave packet solely consists of two plane waves [5-8]. As is well known, this non-regular behavior of the charged particles may yield undesirable effects in a number of technological devices such as the destruction of magnetic surfaces in tokamaks [9]. Thus, in the context of plasma physics *inter al.*, it is natural to consider the problem of regularization of the chaotic dissipative dynamics of a charged particle in a wave packet by a *small* amplitude uncorrelated wave, which is added to the initial wave packet. This Letter studies the simplest model equation to examine this problem:

$$\begin{aligned}\ddot{x}+\gamma\dot{x} &= -\frac{e}{m}\left[E_0\sin\left(k_0x-\omega_0t\right)+E_c\sin\left(k_cx-\omega_ct\right)\right] \\ &\quad -\frac{e}{m}E_s\sin\left(k_sx-\omega_st-\Psi\right), \qquad (1)\end{aligned}$$

where the amplitudes E_0, E_c, E_s, wave numbers k_0, k_c, k_s, and frequencies $\omega_0, \omega_c, \omega_s$ correspond to the "main", chaos-inducing, and chaos-suppressing waves, respectively, Ψ is an initial phase, e and m are the charge and mass of the particle, respectively, and where *weak* dissipation ($\gamma \ll 1$) and *non-uniform* amplitudes ($E_{c,s}/E_0 < 1$) are assumed. In a reference frame moving along with the main wave, Eq. (1) transforms into the equation

$$\begin{aligned}\frac{d^2\xi}{d\tau^2}+\sin\xi &= -\delta-\eta\frac{d\xi}{d\tau}-\varepsilon_c\sin\left(K_c\xi-\Omega_c\tau\right) \\ &\quad -\varepsilon_s\sin\left(K_s\xi-\Omega_s\tau-\Psi\right), \qquad (2)\end{aligned}$$

where $\xi \equiv k_0x-\omega_0t$, $\Omega_0 \equiv \left(ek_0E_0/m\right)^{1/2}$, $\tau \equiv \Omega_0 t$, $\delta \equiv \gamma\omega_0\Omega_0^{-2}$, $\eta \equiv \gamma\Omega_0^{-1}$, $\varepsilon_{c,s} \equiv E_{c,s}/E_0$, $K_{c,s} \equiv k_{c,s}/k_0$, and $\Omega_{c,s} \equiv \left(\omega_{c,s}-\omega_0k_{c,s}/k_0\right)\Omega_0^{-1}$ are all dimensionless variables and parameters. Also, $\Omega_s/\Omega_c = K_sv_{0s}/\left(K_cv_{0c}\right) = \lambda_cv_{0s}/(\lambda_sv_{0c})$, where $v_{0c}\,(v_{0s})$ and $\lambda_c\,(\lambda_s)$ are the relative phase velocity with respect to the main wave ($v_{0c,s} \equiv \omega_{c,s}/k_{c,s}-\omega_0/k_0$) and the wavelength of the chaos-inducing (-suppressing) wave, respectively. The parameters k_0, ω_0, E_0, and Ω_0 are held constant throughout. Physically, Eq. (2) can be used to describe a number of important problems in plasma physics: the dissipative dynamics of a charged particle in the field of three electrostatic plane waves, the bounce dissipative motion of a charged particle trapped in a toroidal magnetic field which is perturbed by two (one chaos-inducing and the other chaos-suppressing) superposed electrostatic waves, and the suppressory effect of a (secondary) resonant magnetic perturbation on the destruction of magnetic surfaces by a (primary) resonant magnetic perturbation in a tokamak. Since Eq. (2) represents a perturbed pendulum ($0 < \delta, \eta, \varepsilon_c, \varepsilon_s \ll 1$), one can apply Melnikov's method (MM) [10,11,2] to obtain analytical estimates of the ranges of parameters (E_s, k_s, ω_s, Ψ) for suppression of the chaos existing in the absence of the chaos-suppressing wave. The application of MM to Eq. (2) gives [12] the Melnikov function

$$M^{\pm}\left(\tau_0\right) = -D^{\pm}+A^{\pm}\sin\left(\Omega_c\tau_0\right)+B^{\pm}\sin\left(\Omega_s\tau_0+\Psi\right), \qquad (3)$$

with $D^{\pm} \equiv 8\eta \pm 2\pi\delta$, $A^{\pm} \equiv 4\varepsilon_cL^{\pm}\left(K_c,\Omega_c\right)$, $B^{\pm} \equiv 4\varepsilon_sL^{\pm}\left(K_s,\Omega_s\right)$, and $L^{\pm}\left(K,\Omega\right) \equiv$

$\pm\int_0^\infty \operatorname{sech}\tau\cos\left[2K\arctan\left(\sinh\tau\right)\mp\Omega\tau\right]d\tau$ (see Fig. 1), where the positive (negative) sign refers to the top (bottom) homoclinic orbit of the underlying conservative pendulum. It is straightforward to obtain the following properties: (*i*) $L^+(K,\pm\Omega)=-L^-(K,\mp\Omega)$; (*ii*) $L^+(K,\Omega)$ vanishes completely in the region $(K,\Omega<0)$ but in a very narrow neighborhood of the line $\Omega=0$; (*iii*) There exists a particular relationship, $\Omega=\alpha K$ with $\alpha\simeq\left(1+\sqrt{5}\right)/2$ (i.e., the *golden ratio*), which determines the direction of the main tongue-like region where $L^+(K,\Omega)$ presents its *largest* values (i.e., for small K values); (*iv*) $L^\pm(K=0,\Omega)=(\pi/2)\operatorname{sech}(\pi\Omega/2)$, $L^\pm(K=n,\Omega=0)=0, n=1,2,...$; and (*v*) $L^\pm(K,\Omega)\in[-\pi/2,\pi/2]$, $\forall(K,\Omega)$. It is well known that the simple zeros of the Melnikov function imply transversal intersection of stable and unstable manifolds, giving rise to Smale horseshoes and hence hyperbolic invariant sets [11]. The mechanism for taming chaos by an added weak periodic perturbation is then the frustration of a homoclinic (or heteroclinic) bifurcation [13]. Consider first the case with no chaos-suppressing wave ($E_s=0$). With fixed $\delta,\eta,\varepsilon_c$, one sees that for *sufficiently* small values of k_c the best chance for the occurrence of a homoclinic bifurcation, i.e.,

$$\frac{|2\eta\pm\pi\delta/2|}{\varepsilon_c}<\left|L^\pm(K_c,\Omega_c)\right|, \tag{4}$$

takes place when $|v_{0c}|$ is close to $|v_{0c,\max}|$, where $v_{0c,\max}=\pm\alpha\Omega_0/k_0$ is the *most chaotic* relative phase velocity (cf. properties (i) and (iii)). Figure 2 shows an illustrative example of this prediction, where the MM-based approximation (top panel) is compared with Lyapunov exponent (LE) calculations of Eq. (2) (bottom panel). One sees that the largest values of the maximal LE (black points) lie inside a narrow tongue-like region which is near the theoretical estimate $\Omega=\alpha K$ (yellow line in Fig. 2). Note that the maximal (positive) LE increases as K_c is increased, which is coherent with the corresponding growth of the chaotic threshold function $|L^+(K,\Omega)|$. With fixed $\delta,\eta,\varepsilon_c$, chaotic motion is possible when $\Omega_c=0$ (i.e., when the relative phase velocity vanishes) and $k_c\neq nk_0, n$ positive integer (cf. property (*iv*), although this possibility decreases as $\lambda_c\rightarrow 0$. Also, as expected, property (i) means that the chaotic threshold depends on the absolute value of the relative phase velocity, but not on its *sign* (cf. Eq. (4)). Let us suppose in the following that, in the absence of any chaos-suppressing wave ($E_s=0$), the associated Melnikov function $M_0^\pm(\tau_0)=-D^\pm+A^\pm\sin(\Omega_c\tau_0)$ changes sign at some τ_0, so that the charged particle exhibits (at least transient) chaotic behavior. To study the taming effect of the chaos-suppressing wave in the most favorable situation, the case of a subharmonic ($\Omega_s=p\Omega_c, p$ a positive integer) resonance is analyzed below. For this case, one has

$$\frac{v_{0s}/v_{0c}}{\lambda_s/\lambda_c}=p, \tag{5}$$

which permits one to identify *two different physical situations (or mechanisms)* for the added chaos-suppressing wave to tame chaotic charged particles: I. Chaos-inducing and chaos-suppressing waves having both *commensurate* wavelengths ($\lambda_s/\lambda_c=m/n, m,n$ positive integers) and *commensurate* relative phase velocities ($v_{0s}/v_{0c}=m'/n', m',n'$ positive integers) such that $p=m'n/(n'm)$. II. Chaos-inducing and chaos-suppressing waves having both *incommensurate* wavelengths and *incommensurate* relative phase velocities such that the quotient $(v_{0s}/v_{0c})/(\lambda_s/\lambda_c)$ satisfies Eq. (5).

Let $\Omega_s=p\Omega_c$, p a positive integer, such that the relationships $\Psi=\Psi_{opt}\equiv\pi[4m+3-p(4n+1)]/2$, $\pi[4m+5-p(4n+1)]/2$, $\pi[4m+3-p(4n-1)]/2$, $\pi[4m+5-p(4n-1)]/2$ are independently satisfied for some positive integers m and n for the parameter regions (K,Ω) where $[L^\pm(K_c,\Omega_c)>0, L^\pm(K_s,\Omega_s)>0]$, $[L^\pm(K_c,\Omega_c)>0, L^\pm(K_s,\Omega_s)<0]$, $[L^\pm(K_c,\Omega_c)<0, L^\pm(K_s,\Omega_s)>0]$, and $[L^\pm(K_c,\Omega_c)<0, L^\pm(K_s,\Omega_s)<0]$, respectively. Then the frustration of a homoclinic bifurcation occurs (i.e., $M^\pm(\tau_0)$ always has the same sign) if and only if the conditions

$$\begin{aligned}
\varepsilon_{s,\min}^\pm &< \varepsilon_s\leqslant\varepsilon_{s,\max}^\pm,\\
\varepsilon_{s,\min}^\pm &\equiv \left(1-\left|D^\pm/A^\pm\right|\right)R^\pm,\\
\varepsilon_{s,\max}^\pm &\equiv R^\pm/p^2,\\
R^\pm &\equiv \varepsilon_c\left|L^\pm(K_c,\Omega_c)/L^\pm(K_s,\Omega_s)\right|
\end{aligned} \tag{6}$$

are fulfilled for each region (K,Ω), respectively. (The proof will be given elsewhere [12].)

Now one can make the following remarks. First, for the above (K,Ω) regions, this result requires having ($\Psi=\pi,\pi/2,0,3\pi/2$), ($\Psi=0,3\pi/2,\pi,\pi/2$), ($\Psi=0,\pi/2,\pi,3\pi/2$), ($\Psi=\pi,3\pi/2,0,\pi/2$), respectively, for $p=4m-3,4m-2,4m-1,4m$ ($m=1,2,...$), respectively in each case. Second, the effectiveness of the chaos-suppressing wave decreases as the resonance order p is increased (cf. Eq. (6)). This is relevant in experimental realizations of the control where the *main* resonance case is then expected to be the most favorable to reliably tame the chaotic dynamics. Third, for the main resonance case ($\Omega_s=\Omega_c$), one has a more accurate and complete estimate [14] of the regularization boundary in the $\Psi-\varepsilon_s$ parameter plane:

$$\varepsilon_s^\pm=\left\{\mp\cos\Psi\pm\sqrt{\cos^2\Psi-\left[1-\left(D^\pm/A^\pm\right)^2\right]}\right\}R^\pm, \tag{7}$$

for $B^\pm>0$ and $A^\pm$, respectively, and

$$\varepsilon_s^\pm=\left\{\pm\cos\Psi\pm\sqrt{\cos^2\Psi-\left[1-\left(D^\pm/A^\pm\right)^2\right]}\right\}R^\pm, \tag{8}$$

for $B^\pm<0$ and $A^\pm$, respectively. The two signs before the square root apply to each of the sign superscripts of $\varepsilon_s^\pm$, which, in its turn, is independent of the sign of $D^\pm$. Also, the area enclosed by the boundary

functions is given by $4\left(\left|D^{\pm}/A^{\pm}\right|\right)R^{\pm}$. The relevance of the above theoretical results on strange chaotic attractor elimination is confirmed by means of LE calculations of Eq. (1) [15]. Figure 3 shows the results corresponding to an illustrative example of the mechanisms of type I (top) and type II for the main resonance case ($p=1$). In the absence of the chaos-suppressing wave ($\varepsilon_s=0$), Eq. (1) presents a strange attractor with a maximal LE $\Lambda^{+}\left(\varepsilon_s=0\right)=0.073\pm0.001$ (bits/s). The diagrams in this figure were constructed by only plotting points on the grid when the respective LE was larger than 0 (cyan points) or than $\Lambda^{+}\left(\varepsilon_s=0\right)$ (magenta points), and with the black dashed-line contour denoting the theoretical boundary function (cf. Eq. (7)) which is symmetric with respect to the optimal suppressory value $\Psi_{opt}=\pi$. Regarding the mechanism of type I, one typically finds that complete regularization $\left(\Lambda^{+}\left(\varepsilon_s>0\right)\leqslant0\right)$ mainly appears inside the island which *symmetrically* contains the theoretically predicted area, while regularization by a type II mechanism seems to be *insensitive* to the initial phase Ψ. In this latter case, the lowest value $\varepsilon_{s,\min}^{+}$ of the theoretical boundary function roughly coincides with the regularization threshold value. The regularization regions in the $\Psi-\varepsilon_s$ parameter plane under the two types of mechanisms present different features. For type I, one typically finds that inside the regularization area which contains the predicted area, the two non-null LEs are *identical and constant* ($\Lambda^{+}=\Lambda^{-}=-\gamma/2$), as is shown in the instance of Fig. 4 (top panel). This *symmetry* property of the contraction of the phase space volume for the predicted regularization areas in the $\Psi-\varepsilon_s$ parameter plane is an inherent feature of the type I mechanism. This property does not hold for the type II mechanism, since in this case the regularization region is not completely "clean" (there exist isolated points corresponding to chaotic behavior) and furthermore the distribution of the non-null (negative) LEs is not perfectly uniform, as can be appreciated in the instance of Fig. 4 (bottom panel).

In conclusion, the onset of chaotic dissipative dynamics of a charged particle in the field of two plane waves and the effectiveness of an added plane wave in taming that chaos have been theoretically predicted and numerically confirmed. Two suppressory mechanisms were identified: One mechanism requires chaos-inducing and chaos-suppressing waves to have both commensurate wavelengths and commensurate relative phase velocities, while the other allows chaos to be tamed when these quantities are incommensurate. A more detailed discussion of the regularization routes by the two mechanisms for the main and higher resonances ($p>1$) as well as of the Hamiltonian limiting case will be given elsewhere [12]. It should be stressed that the results discussed in this work can be directly applied to the problem of the chaos-induced destruction of magnetic surfaces in tokamaks besides other important problems in plasma physics.

---

[1] R. Z. Sagdeev, D. A. Usikov, and G. M. Zaslavsky, *Nonlinear Physics: From the Pendulum to Turbulence and Chaos* (Harwood Academic Publishers, New York, 1988).

[2] A. J. Lichtenberg and M. A. Lieberman, *Regular and Chaotic Motion* (Springer, New York, 1993).

[3] B. V. Chirikov, Phys. Rep. **52**, 263 (1979); W. Wenzel, O. Biham, and C. Jayaprakash, Phys. Rev. A **43** (12), 6550 (1991); A. A. Chernikov *et al.*, Phys. Rev. A **40** (7), 4072 (1989); Y. Nomura, W. Horton, and Y. H. Ichikawa, Phys. Rev. A **45** (2), 1103 (1992); C. Ciubotariu, L. Bădeliţă, and V. Stancu, Chaos, Solitons and Fractals **13**, 1253 (2002).

[4] *Hamiltonian Dynamical Systems – A Reprint Selection*, edited by R. S. MacKay and J. D. Meiss (Adam Hilger, Bristol, 1987).

[5] A. B. Rechester and T. H. Stix, Phys. Rev. A **19**, 1656 (1979).

[6] D. F. Escande, Physica Scripta **T2/1**, 126 (1982).

[7] Y. Gell and R. Nakach, Phys. Rev. A **34**, 4276 (1986).

[8] G. M. Zaslavsky, R. Z. Sagdeev, D. A. Usikov, and A. A. Chernikov, *Weak Chaos and Quasi-Regular Patterns* (Cambridge University Press, Cambridge, 1991).

[9] T. S. Hahn and K. H. Burrell, Phys. Plasmas **2**, 1648 (1995); Z. Lin *et al.*, Science **281**, 1835 (1998).

[10] V. K. Melnikov, Tr. Mosk. Ova. **12**, 3 (1963) [Trans. Moscow Math. Soc. **12A**, 1 (1963)].

[11] J. Guckenheimer and P. Holmes, *Nonlinear Oscillations, Dynamical Systems, and Bifurcations of Vector Fields* (Springer, New York, 1983).

[12] R. Chacón (unpublished).

[13] R. Chacón, Phys. Lett. A **257**, 293 (1999).

[14] R. Chacón, Eur. Phys. J. B **30**, 207 (2002).

[15] It is worth mentioning that one cannot expect too good a quantitative agreement between the two kinds of results for *arbitrary* parameters because LE provides information concerning solely steady chaos, while MM is a perturbative method generally related to transient chaos. It is expected that MM-based predictions should be reliable for *sufficiently* weak perturbative terms.

Figure Captions

Figure 1 (color online). Function $L^{+}(K,\Omega)$ (see the text).

Figure 2 (color online). Top panel: Contour plot of the threshold function $|L^{+}(K,\Omega)|$ with a gray scale from white (1.0 contour) to black (0.0 contour). Bottom panel: Grid of 200×200 points in the $K_c - \Omega_c$ parameter plane where cyan, magenta, and black points indicate that the respective LE was larger than 0.0, 0.07, and 0.14, respectively. System parameters: $\delta = \eta = 0.1, \varepsilon_c = 0.7$.

Figure 3 (color online). Grids of 100×100 points in the $\Psi - \varepsilon_s$ parameter plane for the mechanisms of type I (top panel, $k_s = k_c, v_{0s} = v_{0c}$) and type II (bottom panel, $k_s = \left(\sqrt{5}-1\right) k_c/2, v_{0s} = \left(\sqrt{5}+1\right) v_{0c}/2$. Black dashed-line contour indicates the predicted boundary (cf. Eq. (7)). System parameters: $k_0 = \omega_0 = \Omega_0 = 1, \Omega_s = \Omega_c, \varepsilon_c = 0.7, k_c = 1.22, \omega_c = 2.26, \gamma = 0.1$.

Figure 4. Top panel: Maximal LE Λ^{+} vs the initial phase Ψ for six values of the suppressory amplitude $\varepsilon_s = 0.2, 0.4, 0.6, 0.8, 1.0, 1.2$ corresponding to the type I mechanism. Bottom panel: Maximal LE Λ^{+} vs suppressory amplitude ε_s for six values of the initial phase $\Psi = \pi/3, 2\pi/3, \pi, 4\pi/3, 5\pi/3$ corresponding to the type II mechanism. Dashed-line contour indicates the predicted boundary (cf. Eq. (7)). System parameters as in the caption to Fig. 3.

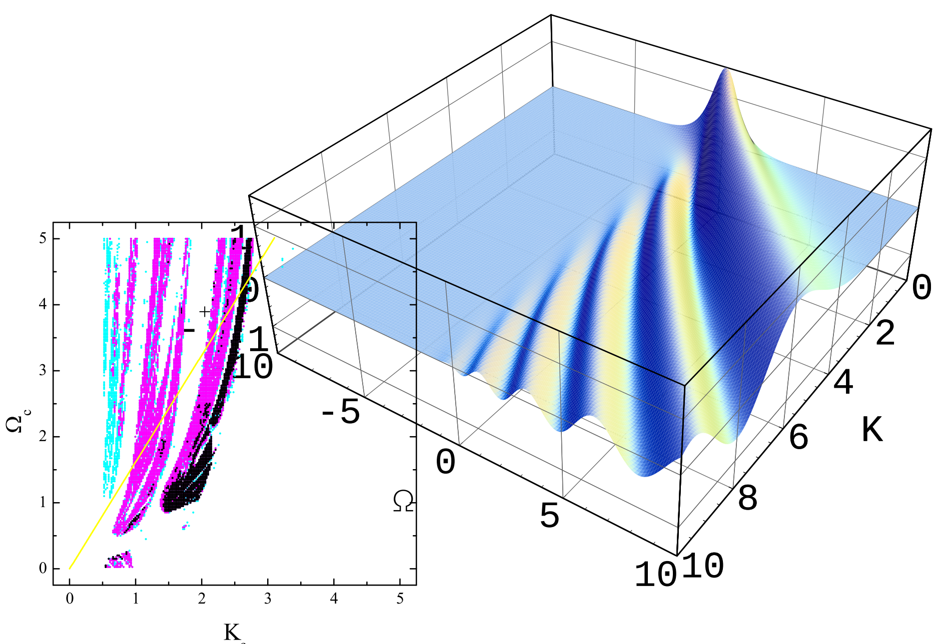

Ω_c
K_c
Ω
K

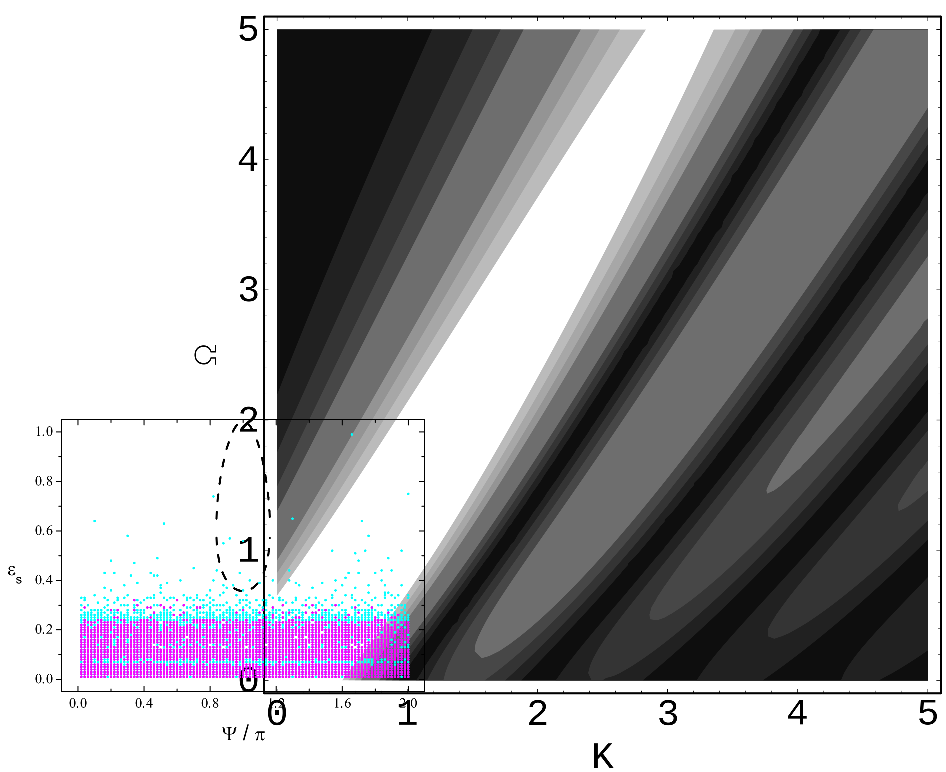

Ω
K
ε_s
Ψ / π

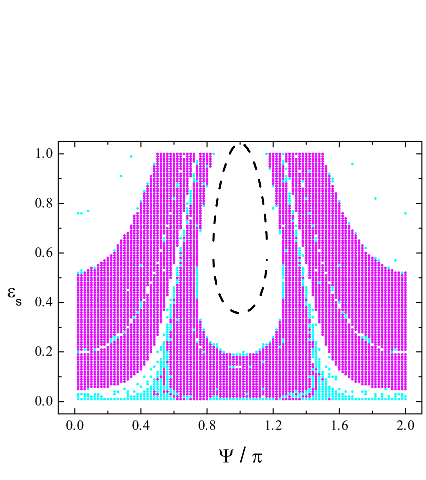

1.0
0.8
0.6
0.4
0.2
0.0
ε_s
0.0
0.4
0.8
1.2
1.6
2.0
Ψ / π

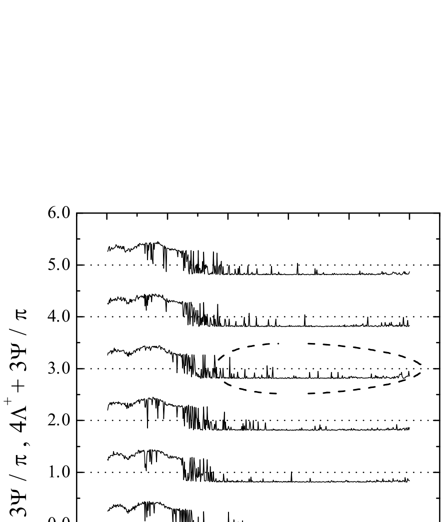

6.0
5.0
4.0
3.0
2.0
1.0
0.0
-1.0
0.0
0.2
0.4
0.6
0.8
1.0
ε_s
$3\Psi / \pi$, $4\Lambda^+ + 3\Psi / \pi$

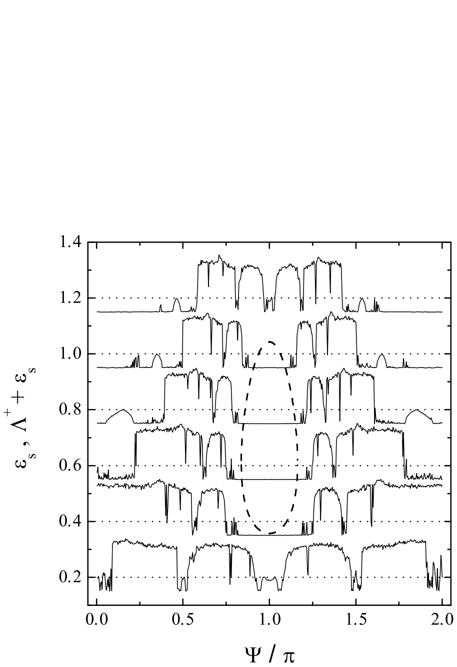

1.4
1.2
1.0
0.8
0.6
0.4
0.2
0.0
0.5
1.0
1.5
2.0
ε_s , Λ⁺ + ε_s
Ψ / π